Aerodynamic Modelling for Integrated Loads Analysis Models

Thiemo M. Kier*

DLR, Institute of Robotics and Mechatronics, 82234, Wessling

Abstract

Loads Analysis is an important discipline in the course of aircraft certification. The loads produced are used to size the structure and have therefore a major impact on the weight of the aircraft. The maximum loads, the so called loads envelope, has to be comprehensive, i.e. all possible scenarios an aircraft can encounter in service life have to be covered. Therefore an immense amount of simulations, so called load cases, is necessary to produce such an envelope. An overview of the load cases defined in the certification specifications CS-25 will be provided. The construction of a simulation model, with its major components, structural dynamics, equations of motion, flight control system and aerodynamics is discussed.

Because of the number of simulations, fast aerodynamic methods need to be employed. The derivation of these methods, along with the simplifying assumptions is outlined. The important concept of Aerodynamic Influence Coefficient (AIC) matrices, which contain gradient information due to a local change in angle of attack is introduced. Two example load cases, a dynamic yawing manoeuvre and a discrete gust encounter are simulated.

Because of the simplifying assumptions, corrections of the AIC matrices with high order methods need to employed. The objective is to use the emerging capabilities of the CFD community to provide aerodynamic data in the high angle of attack regime, and to establish a link and exchange of ideas between the loads and CFD community.

1 Introduction

Loads analysis is an important discipline in the design of an aircraft. For the certification of large airplanes according to CS 25, it has to be demonstrated that the airframe can withstand the loads acting on it within a given flight envelope. In order to size the structure accordingly, a so called loads envelope has to be computed. This loads envelope is comprised of so called load cases, i.e. critical combinations of flight points (viz. altitude, Mach number), mass configurations and specified excitations like design manoeuvres and gusts. The number of conditions to be examined can easily exceed several 100.000s. Clearly such a large number of cases is,

*Research Engineer.

and probably will remain for a while, out side of the scope of high fidelity CFD computations, despite the impressive advances in computing technology.

Therefore, usually much simpler aerodynamic methods based on potential flow theory are employed. These methods are still in use today, because of the relatively cheap computational cost and their ease of use. Further, they provide not only a pressure distribution for a given flight condition, but also the gradient information in terms of so called Aerodynamic Influence Coefficient (AIC) matrices for quasi-steady, as well as unsteady flow regimes. This allows accounting for flexible deformations of the aircraft structure in a very convenient way. An overview of the integration of loads analysis models, along with examples of applications for dynamic manoeuvre and discrete gust calculations will be provided.

However, due to simplifying assumptions in the course of the derivation of the governing equations of the potential theory, important features of the flow, like nonlinearities of control surface efficiencies, transonic effects, or separation can not be captured. These are usually accounted for, by corrections of the AIC matrices with CFD computations. The flight points required for loads analysis are rather untypical for classical CFD computations, where the main focus is on performance around the cruise condition. The capabilities to compute the flow in the corners of the flight envelope, e.g. pulling 2.5 g at Mach numbers of 0.96, are currently emerging and provide invaluable information for the loads community.

2 Loads Analysis

The structural weight of an aircraft is directly related to the loads it has to be designed for. Therefore, loads analysis plays an important role in all design stages. From conceptual, over preliminary, to detailed design for certification, loads have to be determined with an appropriate level of detail. Even past the design stage, loads have to be computed for incidence investigations, e.g. when aircraft in service encounter severe turbulence.

Aeroelastic effects are important and need to be considered. Since the stiffness properties change, when a structure is sized, an iterative process is established until convergence is reached. These are the so called loads loops. This interdependence of several disciplines is characterized by Collars triangle [1], with inertia, stiffness, aerodynamics as vertices, cf. [2]. The advent of electronic fly-by-wire flight control systems (FCS) added an extra vertex, that extends the aeroelastic triangle to a aeroservoelastic tetrahedron.

To determine the maximum loads that occur in the operation of the aircraft, the entire flight envelope has to be covered. While for conventional aircraft the stiffness remains unchanged, the number of investigated mass cases can easily exceed several hundreds, covering different payloads, defuelling sequences with extreme fore and aft c.g. positions in order to represent the operational limits of the aircraft. The aforementioned control laws might have different modes of operation (e.g. normal law, alternate law, direct law, etc.) and loads relevant features like α-protections, gust and manoeuvre load alleviation functions. Aerodynamic data has to be calculated for all configurations, clean, several high lift configurations, each in combination with deployed air-brakes. Further, this data needs to be available for all possible flight conditions in the envelope, i.e. not only around the cruise point, but also for high C_L at high speeds. Several permutations of yaw, pitch, roll rates, angles of attack and separate control surface deflections including spoilers need to be considered.

Further, loads analysis requires quasi-steady aerodynamics for slow manoeuvres, as well as unsteady aerodynamics. Time accurate unsteadiness is of importance, either in simulation of gusts or fast manoeuvres, to account for rapidly changing flow conditions to satisfy the

Kelvin-Thompson Law $\frac{\mathrm{d}\Gamma}{\mathrm{d}t} = 0$.

Design conditions are specified in CS-25 [3]. These conditions can be determined as static trim cases and dynamic manoeuvres, simulated in the time domain, as well as gust and turbulence encounters, usually computed in the frequency domain.

The simplest, and also one of the most important design conditions is the static symmetrical balanced manoeuvres (CS 25.331(b)), where the load factors n_z (positive 2.5g, negative 0g or -1g) are determined according to flight manoeuvering envelope, the so called V-n diagram (figure 1). Important to note is that a vertical balanced manoeuvre results in a nonzero pitch rate, i.e. there is a changing onset angle of attack along the body x-axis.

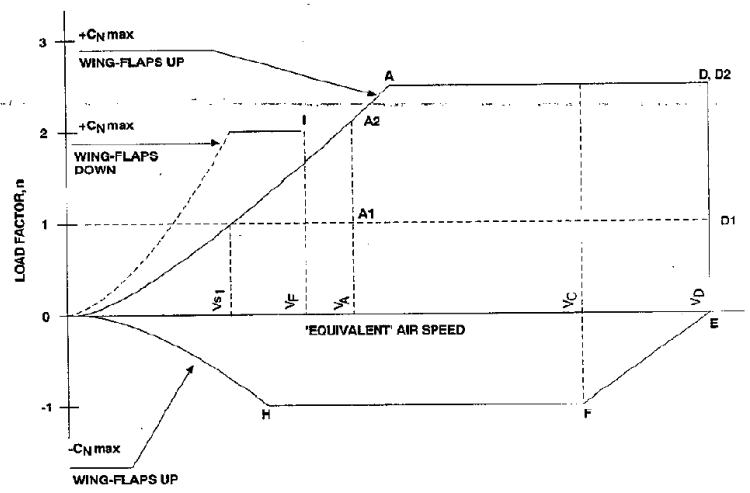

Figure 1: V-n diagram according to CS 25.333 (taken from ref. [3])

Further, there are checked and unchecked symmetrical manoeuvres (CS 25.331(c)), roll manoeuvres (CS 25.349) initiated with positive (1.67g) and negative (0g) load factors with a steady roll rate or a roll acceleration. Roll manoeuvres can be determined statically or dynamically, depending if dynamic effects are present. Dynamic lateral manoeuvres such as one-engine-out (CS 25.367) or yawing manoeuvres (CS 25.351) are significantly influenced by the control laws (active yaw damper). Unsteady aerodynamics are required for discrete gust and turbulence simulations. The discrete gust (CS 25.341(a)) is defined by a 1-cosine shape with a gradient length between 30 and 350 ft. The process of finding the worst case gradient length is referred to as gust tuning. Continuous turbulence (CS 25.341(b)) is defined by a power spectral density [4], and therefore usually computed in the frequency domain if no major nonlinearities are present.

Additional to the flight load conditions covered so far, there are ground load conditions, which are equally important for the sizing of the structure. Those include several landing conditions (also dynamic landing), taxiing, dynamic braking, turning, etc. These are not covered here, since many of those cases do not require aerodynamics.

The number of load cases that need to be calculated to determine the loads envelope can be enormous, since all important permutations of flight points, configurations, mass cases, control laws and manoeuvre and gust conditions need to be considered. Hence, very fast models are a fundamental requirement. The next sections will cover the basic build up of such loads analysis models and the necessary simplifications. A process for building aircraft models for different flight dynamics simulations, including loads analysis is presented in reference [5].

3 Structural Dynamics and Equations of Motion

The starting point, when setting up the equations of motion for a loads analysis model of a flexible aircraft is a Finite Element Model (FEM). This FEM usually consists of 100.000s of degrees of freedom (DoFs), therefore the first step is to statically condense it to reduce the problem size. The method employed is known as the Guyan reduction[6], where condensation points ($g-set$) are placed along a loads reference axis. The mass distributions are prepared for the corresponding payload/fuel cases and connected to the $g-set$. Subsequently, a modal analysis is carried out and only part of the modal basis is retained to further reduce the computational cost.

The eigenvalues and eigenvectors define the generalized coordinates of the $h-set$. The zero eigenvalues represent the rigid body motion. In the case of a full model, the $h-set$ can be explicitly partitioned into six rigid body DoFs ($b-set$) and a flexible part ($f-set$). The rigid body mode shapes $\mathbf{\Phi}_{gb}$ and the retained modes of the eigenvector matrix $\mathbf{\Phi}_{gf}$ are used to generalize the mass and stiffness matrix. The equations of motion are then given in the frequency domain by

$$\left\{-\omega^2\begin{bmatrix}\mathbf{M}_{bb} & \mathbf{0}\\ \mathbf{0} & \mathbf{M}_{ff}\end{bmatrix} + \mathrm{j}\,\omega\begin{bmatrix}\mathbf{0} & \mathbf{0}\\ \mathbf{0} & \mathbf{B}_{ff}\end{bmatrix} + \begin{bmatrix}\mathbf{0} & \mathbf{0}\\ \mathbf{0} & \mathbf{K}_{ff}\end{bmatrix}\right\}\begin{bmatrix}\mathbf{u}_b\\ \mathbf{u}_f\end{bmatrix} = \begin{bmatrix}\mathbf{\Phi}_{gb}^{\mathrm{T}}\\ \mathbf{\Phi}_{gf}^{\mathrm{T}}\end{bmatrix}\mathbf{P}_g^{ext}(\omega), \tag{1}$$

where $\mathbf{u}$ refers to the "displacement" degrees of freedom and $\mathbf{P}$ to the "load" degrees of freedom. It is important to note that DoFs can contain not only the translational, but also the linearized rotational degrees of freedom. The structural $g-set$ for instance consists of six DoFs per grid point, i.e. $\mathbf{P}_g$ is a vector with the three forces and three moments per grid point resulting in a vector length of 6 times number of structural grid points.

A suitable set of equations of motion to account for large rigid body motions and linear flexibility is derived in the references[7, 8, 9, 10]. The nonlinear equations of motion describe the movement relative to a "mean axes" body reference frame. Equations of motion for an unrestrained flexible aircraft accounting for large rigid body motions are given by

$$\begin{aligned}\begin{bmatrix}\mathbf{m}_b\left(\dot{\mathbf{V}}_b + \mathbf{\Omega}_b \times \mathbf{V}_b - \mathbf{T}_{bE}\,\mathbf{g}_E\right)\\ \mathbf{J}_b\dot{\mathbf{\Omega}}_b + \mathbf{\Omega}_b \times (\mathbf{J}_b\mathbf{\Omega}_b)\end{bmatrix} &= \mathbf{\Phi}_{gb}^{\mathrm{T}}\mathbf{P}_g^{ext}(t)\\ \mathbf{M}_{ff}\ddot{\mathbf{u}}_f + \mathbf{B}_{ff}\dot{\mathbf{u}}_f + \mathbf{K}_{ff}\mathbf{u}_f &= \mathbf{\Phi}_{gf}^{\mathrm{T}}\mathbf{P}_g^{ext}(t),\end{aligned} \tag{2}$$

where $\mathbf{\Phi}_{gb}$ is the rigid body modal matrix about the center of gravity and in directions customary in flight mechanics. $\mathbf{V}_b$ and $\mathbf{\Omega}_b$ are the velocity, respectively angular velocity in the body frame of reference. The matrix $\mathbf{T}_{bE}$ transforms the gravitational vector from an earth fixed E to the body fixed coordinate frame b.

In [11] a discrete gust load calculation was carried out comparing a linear frequency domain approach using equations (1), with a time domain computation using equations given in (2). The results from the frequency domain calculations superimposed with the trim solution were virtually identical to those of the integrated time domain model, proving the validity of the approach. As expected, the nonlinearities in the equations of motion only play a subordinate role for gust responses.

4 Aerodynamic Governing Equations

The derivation of the governing flow equations used in flight loads analysis, along with the associated simplifying assumptions are briefly summarized. Many standard reference texts

assume a steady flow condition early in the derivation of these governing equations. However, since for gust loads time accurate unsteady results are essential, this assumption is imposed last.

The Navier-Stokes equations are comprised of laws of conservation of mass, energy and momentum. Since the momentum is a vector quantity in the spatial domain, this results in five equations, and represent the most general set of equations in fluid dynamics. Unfortunately closed form solutions for the Navier-Stokes equations exist only for very few special cases. The flow around a aircraft geometry has to be solved numerically. Common numerical approaches such as finite volume or finite differences schemes require a spatial mesh not only of the surface but also the surrounding volume, leading to many quantities to be solved for. Not only the solution of this set of equations is a enormous task but also the mesh generation is difficult to automatize. These are the governing equations the CFD community is concerned with, either trying to solve them directly with DNS, or with different levels of modelling the turbulence.

The first simplifying assumption is to cancel the viscous terms. The viscosity of air can be considered small. Typical Reynolds numbers for the flow past aircraft wings are of the order of 10^7 or more, depending on the size and speed of the aircraft. In this situation the viscous effects are essentially confined to thin boundary layers covering the surface, therefore neglecting the viscous terms of the Navier-Stokes-equations outside these boundary layers is justified. However, boundary layers may nevertheless have a global impact on the flow by causing separation [12]. These so called Euler equations can not capture separation and viscous drag anymore.

Next irrotationality is assumed, i.e. no vorticity is generated. Vorticity is related to entropy generation by Crocco's Theorem, cf.[12], i.e. irrotationality equals isentropic flow conditions. This allows the introduction of a velocity potential with the velocity vector $\mathbf{v} = \nabla\Phi$. This greatly simplifies the solution process. These so called Full-Potential equations are still nonlinear, however no strong shocks can be captured, due to the isentropic assumption.

Assuming that the flow is dominated by one direction, i.e. $\frac{\Phi_y}{U_\infty} \ll 1$ $\frac{\Phi_z}{U_\infty} \ll 1$ as is usually the case for a flying aircraft, results in the so called Transonic Small Disturbance (TSD) equation. This step is accompanied by the introduction of the disturbance potential. The TSD equation is still nonlinear and is able to capture local supersonic pockets in the flow. However, problems arise near the stagnation point of bluff bodies, where the flow is significantly deflected from the otherwise dominating direction and the aforementioned assumption is violated.

The TSD equation is now linearized. The resulting unsteady Prandtl-Glauert equation (3) is valid only for purely subsonic or purely supersonic flows, i.e transonic effects can not be captured anymore. This is the equation, most aerodynamic methods used in flight loads analysis is based on.

$$\left(1 - Ma_\infty^2\right)\frac{\partial^2\Phi}{\partial x^2} + \frac{\partial^2\Phi}{\partial y^2} + \frac{\partial^2\Phi}{\partial z^2} - \left(2\frac{Ma_\infty}{a_\infty}\right)\frac{\partial^2\Phi}{\partial x \partial t} - \left(\frac{1}{a_\infty^2}\right)\frac{\partial^2\Phi}{\partial t^2} = 0 \tag{3}$$

This equation can be solved using a Boundary Element Method (BEM), which has the significant advantage that only the surface (boundary) needs to be discretized. This simplifies the mesh generation process considerably.

Further assuming steadiness result in the Laplace equation.

$$\frac{\partial^2\Phi}{\partial x'^2} + \frac{\partial^2\Phi}{\partial y^2} + \frac{\partial^2\Phi}{\partial z^2} = 0, \tag{4}$$

where x' is obtained by a geometrical transformation, known as the Prandtl-Glauert Correction $x' = x/\beta$, where $\beta^2 = 1 - Ma_\infty^2$ If the flow is incompressible, i.e. $\rho = const$, then $\beta = 1$.

Hence, the flow is described by the Laplace equation without the need for an approximative transformation. It is worth mentioning that the derivation of Laplace's equation, in contrast to the Prandtl-Glauert equation, does not require the assumption of small perturbations. It can be derived by merely assuming incompressibility.

5 Aerodynamic Influence Coefficients

The major contribution to the excitation forces $\mathbf{P}_g^{ext}$, along with the loads from the propulsion, stem from the aerodynamics. Classical aerodynamic methods based on potential theory are still the workhorses in aeroelastic modelling. They conveniently provide Aerodynamic Influence Coefficient (AIC) matrices, which can be easily integrated in a closed form with the equations of motion (1) and (2).

The basic methods for determining the AICs for a lifting surface discretization are the Vortex Lattice Method for steady and Doublet Lattice Method for unsteady flows. The methods along with the boundary conditions are briefly summarized. The coupling to the structure, respectively to the time and frequency domain equations of motion is discussed.

5.1 Vortex Lattice Method

The Vortex Lattice Method (VLM)[13] discretizes a lifting surface by trapezoidal shaped elementary wings, so called aerodynamic boxes. The aerodynamic lift is generated by placing a vortex along the quarter chord line of such an aerodynamic box. According to the Helmholtz theorems, vortices must either end at a solid surface, or extend to infinity. Hence, the bound vortex is extended to infinity at both corner points, forming the well known horseshoe shape with its legs pointing in free stream direction. The circulation strength $\mathbf{\Gamma}_j$ of the individual horseshoe vortices is then determined using the Biot-Savart-Law by meeting the flow compatibility condition, i.e. no perpendicular flow $\mathbf{v}_j$ through the solid surface. Further, the Kutta condition has to be met, stating that the flow has to leave the trailing edge smoothly. According to Pistolesi's theorem [14] both conditions can be fulfilled simultaneously, if there is no flow trough a collocation point located at mid span, 3/4 chord. The contributions of the three segments of the horseshoe vortex can be calculated with the Biot-Savart Law. The induced

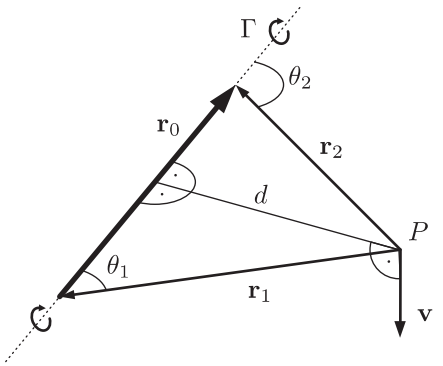

Figure 2: Biot-Savart-Law for a straight vortex filament

velocity for a straight vortex filament with the geometrical properties illustrated in figure 2 is

given by

$$v_t = \frac{\Gamma}{4\pi} \frac{d}{d^2 + r_c^2} \left(\cos\theta_1 - \cos\theta_2\right) \tag{5}$$

for the tangential component, respectively as

$$\mathbf{v} = \frac{\Gamma}{4\pi} \frac{\mathbf{r}_1 \times \mathbf{r}_2}{|\mathbf{r}_1 \times \mathbf{r}_2|^2 + r_c^2 |\mathbf{r}_0|^2} \left(\mathbf{r}_0 \cdot \left(\frac{\mathbf{r}_1}{|\mathbf{r}_1|} - \frac{\mathbf{r}_2}{|\mathbf{r}_2|}\right)\right) \tag{6}$$

for the vector quantity, where r_c is the radius of a viscous core, in order to desingularize the potential vortex for $d = 0$.

Calculating the influence of each horseshoe vortex on every collocation point results in a matrix, which can be inverted to determine the circulations strength when satisfying the flow tangency condition at the collocation points. Normalizing the velocities at the control point with the free stream velocity $\mathbf{w}_j = \frac{\mathbf{v}_j}{U_\infty}$ and using the Kutta-Joukowsky theorem ($L = \rho U_\infty \Gamma b$) to compute pressures from circulation strengths, yields a matrix equation for the differential pressure coefficients with the aerodynamic AIC matrix $\mathbf{Q}_{jj}$.

$$\Delta \mathbf{c}_{\mathbf{p}_j} = \mathbf{Q}_{jj}\ \mathbf{w}_j \tag{7}$$

This is the common implementation for aeroelastic applications used in such codes as NASTRAN [15]. An improved implementation of the VLM is presented in [11], where the Kutta-Joukowsky theorem is calculated using a cross product instead of a scalar multiplication. This method is able to capture additional effects such as induced drag, yaw-roll coupling, etc. which are usually neglected in loads analysis models.

5.2 Doublet Lattice Method

The VLM covers steady aerodynamics at a given instance in time. However, when the normal wash at the collocation points varies, the overall circulation changes. Kelvin's theorem (8) states that this overall circulation within a control volume must remain constant over time.

$$\frac{\mathrm{d}\Gamma}{\mathrm{d}t} = 0 \tag{8}$$

Therefore, when the circulation of the airfoil changes due to the kinematic boundary condition, vorticity of equal strength but opposite sign has to be generated. For an attached flow, this vorticity is shed at the trailing edge and subsequently convected downstream with U_∞, forming a wake vortex sheet with strength γ_w. For slow changes of the normal wash, the influence of shed vorticity in the wake on the airfoil is negligible. If at each time step the normal wash is varied to account for motion of the airfoil, but the effects of the shed vortices are neglected, this is the so called quasi-steady approximation. For fast changing velocities which occur e.g. in gust loads analysis this approximation no longer holds and the modelling of the unsteady aerodynamics becomes necessary. The governing flow equation is the unsteady Prandtl-Glauert equation (3), which differs from its steady counter part (4) by the presence of the partial derivatives wrt to time.

The Doublet Lattice Method[16] (DLM) provides a harmonic solution for this equation. Further, is uses the acceleration potential which is formally equivalent to the velocity potential equation. Therefore, the same elementary solutions are valid, e.g. the source potential. Analogous to acoustics, the harmonically oscillating source is moved wrt a resting fluid, followed by a Gallilei transformation, which moves the observer with the source. Lift can not be generated

by a source, hence the source potential is differentiated wrt the z-direction, yielding the doublet potential. The acceleration potential directly yields the pressure difference between the upper and lower surface, which makes additional steps, i.e. the use of the Kutta-Joukowsky Law, in the load recovery process unnecessary. However, the acceleration potential of the doublet still needs to be integrated to calculate the induced velocity, which is needed to meet the flow tangency condition on the lifting surface. Contrary to the velocity potential of a free flying wing, where there is a velocity jump across the wake surface, there is no such jump in the pressure, hence the wake needs not to be modelled.

The DLM is the unsteady extension to the VLM, which similarly places the singularity along the quarter chord and satisfies the flow tangency at the three quarter chord. The doublet potential is evaluated at discrete points along the quarter chord line, which are used for a polynomial fit and its subsequent analytical integration. The integration still can not be performed in closed form and series approximations for parts of the kernel functions need to be employed. The final result for the pressure coefficient

$$\Delta \mathbf{c_p}_j(k) = \mathbf{Q}_{jj}(k)\mathbf{w}_j(k) \tag{9}$$

has similar form to the conventional steady aerodynamics, where

$$k = \frac{c_{ref}/2}{U_\infty}\omega \tag{10}$$

is the reduced frequency. In fact, for $k = 0$ the DLM solution is replaced by the VLM results[17], since for the steady case no approximations are required.

5.3 Aerodynamic boundary conditions

For the methods mentioned above, the lifting surface are modelled by a flat mean surface approach, i.e. camber and incidence effects are handled purely by the boundary conditions. To calculate the pressure difference, the geometry, motion or gust induced normal wash at the three-quarter-chord point ($j - set$) needs to be determined. The reference point of an aerodynamic box is its mid point and denoted by the $k - set$. The $k - set$ has at least two degrees of freedom, namely z and θ.

The lift acts in the local z-direction at the quarter chord location and therefore creates a local pitching moment about the local y-axis. Multiplication of this transformation with a diagonal matrix of the local box areas, yields the matrix $\mathbf{S}_{kj}$, which converts the pressures to discrete loads at the mid chord location.

To calculate the normal wash at the three-quarter-chord, the rotation about the y-axis ($\mathbf{D^x}_{jk}$) and the heaving motion ($\mathbf{D^t}_{jk}$) need to be considered, i.e. the differentiation wrt the x-direction and wrt time.

$$\mathbf{w}_j(t) = \left(\underbrace{\begin{bmatrix} 0 & 1 \end{bmatrix}}_{\mathbf{D^x}_{jk}} + \frac{\mathrm{d}}{\mathrm{d}t}\left(\frac{c_{ref}/2}{U_\infty}\right) \cdot \underbrace{\frac{2}{c_{ref}}\begin{bmatrix} -1 & c_j/4 \end{bmatrix}}_{\mathbf{D^t}_{jk}} \right) \mathbf{u}_k(t) \tag{11}$$

The matrix $\mathbf{D^t}_{jk}$ is multiplied by $2/c_{ref}$, in order to account for the reduced frequency of equation (10). Hence, the flow conditions can be expressed as a function of reduced frequency, in terms of the displacements of the $k - set$.

$$\mathbf{w}_j(k) = \left(\mathbf{D^x}_{jk} + \mathrm{j}k\, \mathbf{D^t}_{jk}\right)\ \mathbf{u}_k(k) \tag{12}$$

If the the Kutta-Joukowsky theorem is applied as cross product, the $k-set$ needs to be extended to six DoFs and the introduction of a lift acting point becomes necessary. This methodology is described in [11].

5.4 Fluid-Structural Coupling

The aerodynamic properties are given with respect to the aerodynamic grid. The matrix connecting the displacements of the structural $(g-set)$ to the aerodynamic degrees of freedom $(k-set)$ is called spline matrix $\mathbf{T}_{kg}$.

$$\mathbf{u}_k = \mathbf{T}_{kg}\mathbf{u}_g \tag{13}$$

The method employed to create this spline matrix is the commonly used Infinite Plate Spline (IPS) [18], which uses the radial basis function $\phi(r) = \|r\|^2 \ln(\|r\|)$, where r is the euclidian distance between the structural (g-set) and the aerodynamic (k-set) grid. The aerodynamic loads can be mapped back onto the structure with the transpose of the spline matrix.

$$\mathbf{P}_g = \mathbf{T}_{kg}^{\mathrm{T}}\mathbf{P}_k \tag{14}$$

The modal matrix $\mathbf{\Phi}_{gf}$, respectively its transpose connects the flexible part of the EoM (1) and (2) to the aerodynamic model.

Hence, the generalized aerodynamic forces due to flexibility are given as

$$\mathbf{P}_f^{aero} = \mathbf{\Phi}_{gf}^{\mathrm{T}}\mathbf{T}_{kg}^{\mathrm{T}}\mathbf{S}_{kj}\mathbf{Q}_{jj}\ \left(\mathbf{D^x}_{jk} + \frac{\mathrm{d}}{\mathrm{d}t}\left(\frac{c_{ref}/2}{U_\infty}\right)\cdot\ \mathbf{D^t}_{jk}\right)\mathbf{T}_{kg}\mathbf{\Phi}_{gf}\ \mathbf{u}_f, \tag{15}$$

where $\mathbf{u}_f$ is the generalized modal deflections. Substituting (15) in the equations of motion (1) or (2) allow for a closed formulation as a system of ODEs. Also note that the number of retained modes is usually small compared to the structural and aerodynamic degrees of freedom. When the matrix multiplications in eq. (15) are carried out in a preprocessing step, the resulting matrix sizes are reduced tremendously.

In contrast to typical CFD-CSM coupling schemes, there is no need to pass the forces, respectively displacements between two separate applications. This is possible as the AIC matrix $\mathbf{Q}_{jj}$ contains directly the gradient information, due to a local change in the flow tangency boundary condition.

5.5 Time domain unsteady aerodynamics

Gust load calculations are usually computed in the frequency domain. One of the reasons, is the availability of tabulated unsteady aerodynamic matrices as function of reduced frequency through the DLM.

To make the frequency domain unsteady aerodynamics usable for time domain calculations, provision need to be taken. One possibility is to fit the tabulated frequency data with a Rational Function Approximation (RFA). The resulting form can be expressed in the Laplace domain and thus be used for time domain simulations. For a shorter notation, it is convenient to introduce an equivalent to the reduced frequency k in the Laplace domain denoted by $\hat{s} = s\left(\frac{c_{ref}/2}{U_\infty}\right)$.

The RFA captures the time dependent behavior of the unsteady flow by introducing of additional aerodynamic lag states. Many flavors of this method have been published in literature [19, 20, 21, 22]. Most of these publications concentrate on approximation of the generalized

aerodynamic matrices $\mathbf{Q}_{hh}$, i.e. the AIC matrices are already multiplied with the differentiation matrices (12) and the modal basis. While this approach reduces the computational cost considerably due to a smaller problem size, it also has some significant disadvantages. One is that the steady and unsteady aerodynamic contributions can not be discerned anymore. Further, the approximation becomes tied to a mass case, whereas a physical approximation is only dependent on the Mach number.

In [11] a scheme is proposed to approximate directly the physical AIC matrices $\mathbf{Q}_{jj}(k)$, using Roger's method.

$$\mathbf{Q}_{jj}(\hat{s}) = \mathbf{Q^0}_{jj} + \mathbf{Q^1}_{jj}\hat{s} + \sum_{i=1}^{n_p} \mathbf{Q^{L_i}}_{jj} \frac{\hat{s}\mathbf{I}}{\hat{s} + p_i} \tag{16}$$

The term $\mathbf{Q^0}_{jj}$ represents the quasi-steady term, $\mathbf{Q^1}_{jj}$ is the added mass, and the $\mathbf{Q^{L_i}}_{jj}$ with the predefined poles p_i terms are responsible for the lagging behavior of the unsteady flow. Interesting to note is the absence of the $\mathbf{Q^2}_{jj}$ acceleration term in the physical approximation. The reason for the presence of a second derivative in the classical RFA, is the additional time derivative in the downwash equation (12).

The system (16) can be now used for the time domain simulation. Pre-multiplying equation (16) with $\mathbf{T}_{kg}^{\mathrm{T}}\mathbf{S}_{kj}$, the approximation can be expressed in the following form,

$$\mathbf{Q}_{gj}(\hat{s}) = \mathbf{Q^0}_{gj} + \mathbf{Q^1}_{gj}\hat{s} + \mathbf{D}\left(\hat{s}\mathbf{I} - \mathbf{R}\right)^{-1}\mathbf{E}\hat{s} \tag{17}$$

and then be cast in the form of an ordinary differential equation (ODE) for the lag states, with $\dot{\mathbf{w}}_j$ as input.

$$\dot{\mathbf{x}}_L = \mathbf{R}\left(\frac{U_\infty}{c_{ref}/2}\right)\mathbf{x}_L + \mathbf{E}\,\dot{\mathbf{w}}_j \tag{18}$$

When using Roger's method, the involved matrices $\mathbf{R}$ and $\mathbf{E}$ have a pronounced sparsity pattern, such that the ODEs are fully decoupled. The resulting aerodynamic forces are then

$$\mathbf{P}_g^{aero} = \underbrace{\left(\mathbf{Q^0}_{gj}\,\mathbf{w}_j\right)}_{\text{steady } \mathbf{P}_g^s(\mathbf{w}_j)} + \underbrace{\left(\mathbf{Q^1}_{gj}\left(\frac{c_{ref}/2}{U_\infty}\right)\,\dot{\mathbf{w}}_j + \mathbf{D}\,\mathbf{x}_L(\dot{\mathbf{w}}_j)\right)}_{\text{unsteady } \mathbf{P}_g^u(\dot{\mathbf{w}}_j)}. \tag{19}$$

The most significant advantage of this physical RFA over the traditional generalized approximation is that equation (19) can be split explicitly into a steady part depending on $\mathbf{w}_j$ and an unsteady part solely depending on $\dot{\mathbf{w}}_j$. For dynamic manoeuvre simulations the unsteady contribution can be included, e.g. for gust computations or fast manoeuvres, or neglected if deemed unnecessary.

6 Examples

6.1 Dynamic Yawing Manoeuvre

A critical load case for the vertical tailplane (VTP) is the yawing manoeuvre condition.

According to CS 25.351 the yawing manoeuvre can be described as follows:

1. at an unaccelerated trimmed horizontal flight, the rudder control is suddenly displaced to maximum deflection.

2. during the dynamic application of the rudder a overswing results, yielding a maximum sideslip angle.

3. after a steady sideslip angle is reached,

4. the rudder control is returned to a neutral position.

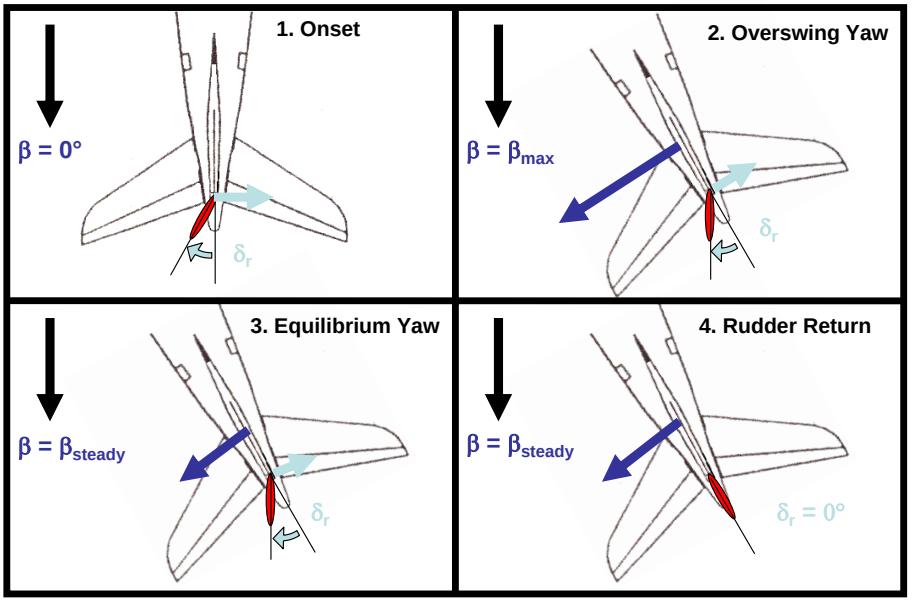

Figure 3: Yawing Manoeuvre according to CS 25.351

When the rudder is deflected a force acting in the direction of yaw is applied. This force acts due to the suction peak of the deflected control surface. Then, as a sideslip angle gradually builds up, a counter force due to β is invoked. The force due to β is located forward compared to the one induced by δ_r, hence a torsional moment is induced. The highest torsional loads occur when the aircraft reaches a maximum sideslip angle β, reached by a dynamic overswing. After a while, an equilibrium is reached and the rudder deflection is returned to zero. The suddenly missing rudder force causes the maximum shear forces and bending moments at this point. The loads are depicted in figure 4. [4]

6.2 Discrete Tuned Gust

Discrete tuned gusts are defined in CS 25.341(a). The velocity profile is defined as a 1-cos shape.

$$v_G = \frac{1}{2} U_{ds} \left(1 - \cos \frac{2\pi x(t)}{2H} \right) \tag{20}$$

The gust gradient H is the distance parallel to the airplane's flight path from the start of the gust to its peak, the design gust velocity U_{ds}. Hence, the total gust length is $2H$. Several gust gradient distances between 30ft and 350ft have to be calculated to find the critical response for each load quantity. This process is called gust tuning.

The gust spectrum of a discrete tuned gust $\mathbf{v}_G(\omega)$ is available semi-analytically in the frequency domain. When the aircraft is subjected to the gust, the penetration speed U_∞ and

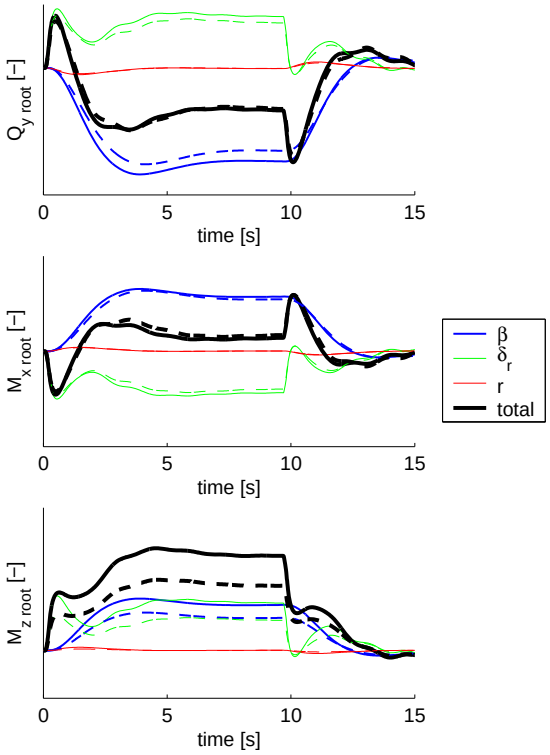

Figure 4: forces and moments at VTP root caused by the different effects

location of the control points $\mathbf{x}_j$ wrt the gust need to be considered. In the frequency domain these time lags are expressed as phase shifts with an exponential function.

$$\mathbf{w}_j^G(\omega) = \mathbf{n}_j \cdot \exp\left(-\mathrm{j}\omega \cdot \mathbf{x}_j / U_\infty\right) \cdot \mathbf{v}_G(\omega)/U_\infty \tag{21}$$

The generalized gust column for the frequency domain can then be set up.

$$\mathbf{Q}_{hG}(k) = \mathbf{\Phi}_{gh}^{\mathrm{T}} \mathbf{Q}_{gj}(k) \mathbf{w}_j^G(\omega) \tag{22}$$

For nonlinear time domain simulations, eq.(21) can simply be expressed as a function of time. The relative location of the airframe wrt the gust is

$$\mathbf{x}_j^G(t) = \mathbf{x}_j + 2H - U_\infty \cdot t. \tag{23}$$

The normalized gust velocities are then given as,

$$\mathbf{w}_j^G(t) = \begin{cases} \frac{1}{2U_\infty}\left(1 - \cos\left(\pi \cdot \frac{\mathbf{x}_j^G(t)}{H}\right)\right) \cdot \mathbf{n}_j, & \text{for} \quad 0 < \mathbf{x}_j^G < 2H \\ 0 & \text{otherwise} \end{cases} \tag{24}$$

Differentiation of the normalized gust velocity wrt time yields,

$$\dot{\mathbf{w}}_j^G(t) = \begin{cases} -\frac{\pi}{2H} \cdot \sin\left(\pi \cdot \frac{\mathbf{x}_j^G(t)}{H}\right) \cdot \mathbf{n}_j, & \text{for} \quad 0 < \mathbf{x}_j^G < 2H \\ 0 & \text{otherwise} \end{cases} \tag{25}$$

In the time domain simulation, the gust excitation becomes merely a function of time when integrating the ODEs. If the velocity of the aircraft is assumed to be constant, the gust is

independent of the aircraft simulation and can be pre-computed as a function of Ma, H and U_∞. Subsequently, the results are fed into the overall aircraft simulations. If the the position relatively to the wind field changes, e.g. in the case of a wake vortex encounter, the influence has to be computed online. Reference [23] shows that depending on the encounter angle, that a mixture of two types of responses are possible. A large manoeuvre type response, where large nonlinear roll angles occur and nonlinear equations of motion (2) are important, or a gust type response, where unsteady aerodynamic effects are present.

Figure 5 shows a comparison of a time domain simulation and frequency domain solution that is transformed to the time domain by an inverse Fourier transform.

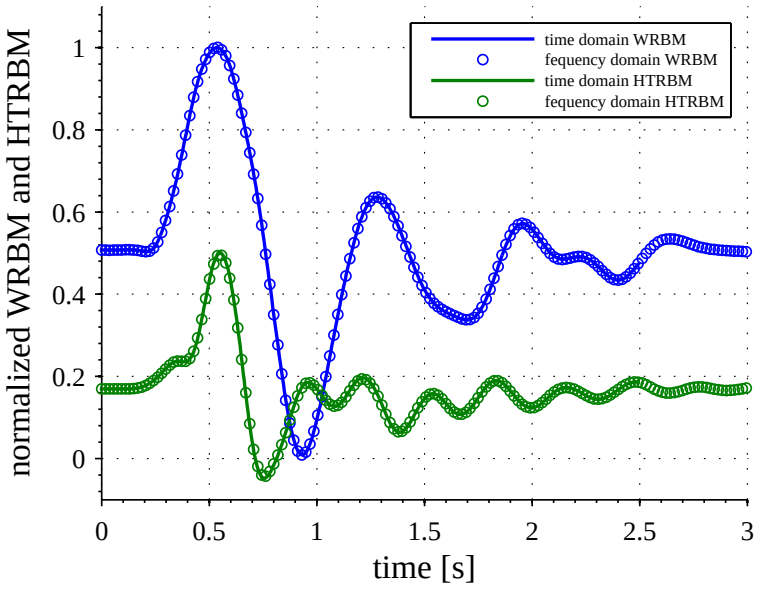

Figure 5: Loads for time and frequency domain solutions

The agreement between the time integration and frequency response calculation is excellent.

7 Corrections for Unmodelled Effects

So far only the theoretical results of the methods based on potential theory were discussed. As already mentioned in the derivation of the governing equation, a lot of important features of the flow can not be captured, such as viscous drag, separation, or shocks to name only a few. Therefore, corrections of the AIC matrices have to be applied. There are numerous proposals including diagonal correction [24] or fully populated matrices [25], which can be applied at force level, by pre-multiplication or at downwash level, by post-multiplication. Corrections are applied to steady, unsteady and/or modal quantities[26][27]. Also direct manipulation of the AIC matrices was suggested [28]. An assessment of correction methods is available in reference [29].

These corrections are applied at various points to cover nonlinearities. Usually, only the angle of attack α as predominant source of the nonlinear behavior is considered. The nonlinear effects associated with control surface effectivities are treated separately, assuming that a scaling factor dependent on angle of attack and deflection is sufficient i.e. the pressure distribution due to deflection remains the same. It should be noted that these corrections are applied about a reference point or shape, around which the linearity assumption must be still valid. That might

result in a large amount of data. Some work [30] commenced to apply reduced order modelling techniques directly to AIC matrices instead of pressure distributions, which lead to promising results.

The prime question is where the correction data is coming from. Typically, a 2.5g pull-up with air-brakes deployed at the stall onset at the V_D/M_D point in the flight envelope is where maximum loads occur. Incidently, this is also the hardest problem for CFD applications. Another difficult problem is at slower speeds, when the local angles of attack induced by a gust exceed the linear regime and dynamic stall effects need to be captured. Usually these issues are tackled by relying on wind tunnel data and conservative assumptions.

At the same time, it needs to be recognized that loads analysis does not require the same level of detail as aerodynamic design, e.g. the accuracy of drag forces are of minor importance, unless they significantly change the overall pitching moment, local regions of back-flow are not important if they only marginally change the sectional lift and moment. Also, while trying to increase the accuracy, there is still need for a certain amount of conservatism in safety critical applications.

CFD-CSM coupled solutions provide important test cases, with which the fast method can be calibrated and validated. Also staggered multi-fidelity approaches are thinkable, were the fast methods are used to scan the envelope and higher fidelity approaches are used to examine the critical load cases in more detail.

8 Conclusions

An overview of the field of loads analysis was given. The construction of loads analysis models was presented including structural dynamics, equations of motion and flight control systems. The main focus was on the aerodynamic modelling and how fast methods are used to cope with the enormous amount of load cases that need to be simulated. Two examples calculations are presented. One dynamic yawing manoeuvre case were nonlinear and FCS effects are important, and a discrete gust, where unsteady aerodynamics are essential.

It is hoped to foster some understanding of the motivations for modelling approaches and requirements in the realm of loads analysis. Loads models have to be fast yet accurate enough to address the needs in aircraft design. The goal is to make use of the emerging capabilities of the CFD community to provide aerodynamic data in the high angle of attack regime by construction of suitable Reduced Order Models or AIC corrections. The aspiration is to establish a link and exchange of ideas between the loads and CFD community.

References

[1] A.R. Collar. The Expanding Domain of Aeroelasticity. *Journal of the Royal Aeronautical Society*, 50:613–636, 1946.

[2] R. L. Bisplinghoff, H. Ashley, R. L. Halfman. *Aeroelasticity.* Dover Publications Inc., 1955.

[3] European Aviation Safety Agency. *Certification Specifications for Large Aeroplanes CS-25*, volume Subpart C - Structure. EASA, 2010.

[4] F. M. Hoblit. *Gust Loads on Aircraft: Concepts and Applications.* AIAA Education Series, 1988.

[5] T. Kier, G. Looye, M. Scharpenberg, and M. Reijerkerk. Process, Methods and Tools for Flexible Aircraft Flight Dynamics Model Integration. In *International Forum on Aeroelasticity and Structural Dynamics*, number IF-060. CEAS/AIAA, 2007.

[6] R. J. Guyan. Reduction of stiffness and mass matrices. *Journal of Aircraft*, 3(2):380, 1965.

[7] M. R. Waszak and D. K. Schmidt. On the flight dynamics of aeroelastic vehicles. In *AIAA Atmospheric Flight Mechanics Conference*, number AIAA 86-2077, pages 120–133. AIAA, 1986.

[8] M. R. Waszak and D. K. Schmidt. Flight Dynamics of Aeroelastic Vehicles. *Journal of Aircraft*, 25(6):563–571, 1988.

[9] M. R. Waszak, C. S. Buttrill and D. K. Schmidt. Modeling and Model Simplification of Aeroelastic Vehicles: An Overview. Technical Report NASA TM-107691, NASA LARC, 1992.

[10] C. Reschke. *Integrated Flight Loads Modelling and Analysis for Flexible Transport Aircraft.* PhD thesis, Universität Stuttgart, 2006.

[11] Kier, T.M. and Looye, G.H.N. Unifying Manoeuvre and Gust Loads Analysis. In *International Forum on Aeroelasticity and Structural Dynamics*, number IFASD-2009-106, 2009.

[12] A. Jameson. Computational Aerodynamics for Aircraft Design. *Science*, 245:361–371, 1989.

[13] S. Hedman. Vortex Lattice Method for Calculation of Quasi Steady State Loadings on Thin Elastic Wings. Technical Report Report 105, Aeronautical Research Institute of Sweden, October 1965.

[14] Pistolesi, E. Betrachtungen über die gegenseitige Beeinflussung von Tragflügelsystemen. In *Gesammelte Vorträge der Hauptversammlung 1937 der Lilienthal Gesellschaft*, 1937.

[15] W.P. Rodden, R.L. Harder, and E.D. Bellinger. Aeroelastic Addition to NASTRAN. Technical Report NASA CR-3094, NASA, March 1979.

[16] E. Albano and W.P. Rodden. A doublet-lattice method for calculating lift distributions on oscillating surfaces in subsonic flows. *AIAA Journal*, 7(2):279–285, 1969.

[17] W.P. Rodden, J.P. Giesing and T.P. Kalman. New developments and applications of the subsonic doublet-lattice method for nonplanar configurations. In *AGARD Symposium on unsteady aerodynamics for aeroelastic analyses of interfering surfaces*, number AGARD-CP-80-71. AGARD, 1971.

[18] R.L. Harder and R.N. Desmarais. Interpolation Using Surface Splines. *Journal of Aircraft*, 9(2):189–191, 1972.

[19] K. L. Roger. Airplane math modeling methods for active control design. In *AGARD Structures and Materials Panel*, number AGARD/CP-228, pages 4–1 – 4–11. AGARD, April 1977.

[20] Edwards, J.W. Applications of Laplace transform methods to airfoil motion and stability calculations. In *20th Structures, Structural Dynamics and Materials Conference*, number AIAA 1979-772, 1979.

[21] I. Abel. An analytical technique for predicting the characteristics of a flexible wing equipped with an active flutter-suppression system and comparison with wind-tunnel data. Technical Report NASA TP-1367, NASA LARC, 1979.

[22] M. Karpel. Design for Active and Passive Flutter Suppression and Gust Alleviation. Technical Report NASA CR-3482, NASA, November 1981.

[23] Kier, T.M. An Integrated Loads Analysis Model including Unsteady Aerodynamic Effects for Position and Attitude dependent Gust Fields. In *International Forum on Aeroelasticity and Structural Dynamics*, number IFASD-2011-052, 2011.

[24] J.P. Giesing, T.P. Kalman and W.P. Rodden. Correction Factor Techniques for Improving Aerodynamic Prediction Methods. Technical Report NASA CR-144967, May 1976.

[25] I. Jadic, D. Hartley, and J. Giri. An Enhanced Correction Factor Technique for Aerodynamic Influence Coefficient Methods. In *MSC Aerospace User's Conference*, 1999.

[26] M.L.. Baker. CFD-Based Correction for Linear Aerodynamic Methods. In *AGARD Symposium on unsteady aerodynamics for aeroelastic analyses of interfering surfaces*, number AGARD-CP-80-71. AGARD, 1971.

[27] P.C. Chen, R.G.A. Silva, and D.D. Liu. Transonic AIC Weighting Method using Successive Kernel Expansion. In *46th AIAA/ASME/ASCE/AHS/ASC Structures, Structural Dynamics and Materials Conference*, number AIAA 2005-1991. AIAA, 2005.

[28] J. Brink-Spalink and J.M. Bruns. Correction of Unsteady Aerodynamic Influence Coefficients Using Experimental or CFD Data. In *International Forum on Aeroelasticity and Structural Dynamics*, 2001.

[29] R. Palacios, H. Climent, A. Karlsson, B. Winzell. Assessment of Strategies for Correcting Linear Unsteady Aerodynamics Using CFD or Test Results. In *International Forum on Aeroelasticity and Structural Dynamics*, 2001.

[30] Judt, D. Model Order Reduction of Aerodynamics for Flight Dynamic Simulations. Master's thesis, University of Glasgow, 2010.